

Research Article

**Modeling and optimizing acid cyanine 5R removal from aqueous solutions
using immobilized MgO nanoparticles on glass**

Mohamadreza Massoudinejad¹ and Reza Nemati^{2*}

¹Member of Safety Promotion and Injury Prevention Research Center ,
And Professor of Environmental Health Engineering, School of Public Health, Shahid Beheshti University of
Medical Sciences, Tehran PO Box: 19835 35511, Iran, Tel. +9821 22432040;

Fax: +982122432036; email: massoudi@sbmu.ac.ir

²PhD student in Environmental Health Engineering,
Department of Environmental Health, School of Public Health,
Shahid Beheshti University of Medical Sciences, Tehran PO Box: 19835 35511, Iran,
Tel. +98 2122432040; Fax: +982122432036

*Corresponding Author: E-mail: reza.neamati@gmail.com

ABSTRACT

In this study, the nanoadsorbents were immobilized on an inert support (glass) to minimize their release to the environment. The initial dye concentration (acid cyanine 5R, an azo dye), pH and contact time parameters were optimized using central composite design under response surface methodology. The experiments were done in a 10 liter glass reactor with MgO nano (as good dye adsorbent) coated glass partitions. COD and dye removal efficiency were determined by assessing before and after the adsorption. The COD removal efficiency and the remaining dye were close-fitting well to the quadratic model in the experimentation range of variables. The experimental study showed that fixed MgO on the glass was effective in AC 5R adsorption. The optimal operating point (initial dye=30 mg l⁻¹, pH= 9 and contact time= 90 min) giving maximum dye and COD removal was found using DesignExpert 7.0.0 software (85% and 83%, respectively).

Keywords: Azo dye, Chemical Oxygen Demand, Silicone adhesive, Textile wastewater.

1. INTRODUCTION

The discharges of untreated industrial waste water play an important role in the emission of pollutants to the environment. Colored effluents from industries such as leather and textile are major environmental challenges because some of the dyes in these effluents are carcinogen and persistent in the environment and can cause other environmental and aesthetical problems (the dyes are visible even at low concentrations ~0.005 ppm)[1, 2]. Within various industries, textile industries are the largest consumers' dyes (about two-thirds of the manufactured dyes)[3]. Typically, the textile industries consume about 130m³ of water per ton of product (Kocabas et

al., 2009). High water consumption leads to producing a high volume of colorful effluent. According to Lu et al. in 2010, textile wastewater treatment and reuse can be possible and economically reasonable (Lu et al., 2010). Textile industry's effluents contain a variety of dyes, which are usually synthetic and have high molecular weight, complex chemical structure and low biodegradability[4]. Therefore, these dyes must be removed using appropriate methods prior to discharge to the environment. Among the various utilized methods, adsorption is a favorable method for the treatment of these wastes because of its

simplicity in design, cost-effective feasibility, recycling of adsorbent and absence of unsafe residues[5]. Adsorption refers to the gathering of an ingredient (adsorbate) at the interface between two phases (liquid–solid interface)[6].

Nanoadsorbents are usually used as the suspended slurry of fine particles in reactors. Although the suspended adsorbent makes a higher surface area for the adsorption and degradation of pollutants and reactors have simple design, this type of reactor has the drawback of low energy utilization and it is difficult to separate or recover the adsorbent after the reaction. To minimize their release to the environment and overcome the disadvantage of the suspended adsorbent-based slurry system for practical applications, nanoadsorbents are immobilized on an inert support (such as glass). These immobilized nanoadsorbents have been synthesized using various chemical methods such as hydrothermal [7], sol–gel[8] and chemical vapor deposition[9].

Recent studies have shown that MgO nanoparticles have significant adsorption capacity for the dye removal of wastewaters because of high surface to volume ratio, great adsorption surface area, large numbers of highly reactive edges and the destructive sorbents[10, 11]. Adsorbates react in adsorption surface and convert into less poisonous compounds, which is known as destructive adsorption[12]. MgO nanoparticles are of the cheapest and most easily prepared adsorbents[13]. Studies have indicated that MgO nanoparticles can be used for the removal of azo

acidic reactive dyes from wastewaters[14]. Azo dyes are an important group of synthetic organic dyes and used in textile industries. They have one or more azo bonds ($N = N$)[15] and constitute more than 60% of the total produced dyes[14].

In this work, the potential efficiency of immobilized MgO nanoparticles in the removal of an azo dye was investigated. However, the immobilization of MgO nanoparticles with the above-listed methods was not successful. Therefore, attempts were made to immobilize MgO nanoparticles using simple adhesives. Initial tests showed that immobilizing MgO nanoparticles on the glass by silicone adhesive was better than other adhesives, such as cyanoacrylate. Therefore, silicone adhesive was used for this purpose. Acid cyanine 5R (AC 5R), an azo dye, was employed as the model dye. Also, chemical oxygen demand (COD) was used as the supplementary index for assessing the treatment efficiency.

2. MATERIALS AND METHODS

2.1 Materials

Magnesium oxide nanoparticles (MgO nanoparticles) with the size of 20 nm, purity of 98% and surface area of $>60 \text{ m}^2\text{g}^{-1}$ were purchased from US-Nano Co. Acid cyanine 5R was obtained from Alvan Sabet Company, Iran. The chemical structure of acid cyanine 5R is shown in Figure 1. Sodium hydroxide and other required compounds such as HCl were procured from Merck, Germany.

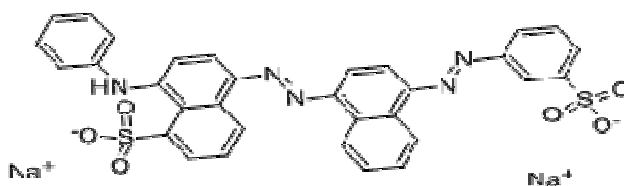


Figure 1 schematic demonstration of the chemical structure of Acid cyanine 5R dye (synonym: Acid Blue 113).

2.2 Sample preparation

The stock solutions at the desired concentration were prepared by liquefying the dye in distilled water. The experimental samples (with the concentrations in the range of $5\text{--}50 \text{ mg l}^{-1}$) were made up by these solutions. The pH of the

sample solutions was adjusted using 0.1N HCl or NaOH solutions. The dye removal experiments were accomplished in a 10 L liter glass batch reactor with MgO nanocoated glass partitions. Each test consisted of preparing the dye solution with the chosen initial

concentration and pH by diluting the stock dye solution by distilled water. After the experiments (with different retention times), the supernatant was analyzed for the residual dye and COD. Efficiency of the dye and COD removal was calculated by the following equation:

Eq. 1 Dye and COD removal efficiency (%) =

$$\frac{C_i - C_e}{C_i} \times 100$$

where C_i indicates the initial AC 5R and initial COD and C_e indicates the end (following adsorption) AC 5R dye concentrations and COD. All the experimentations were done at room temperature and at least three times independently. The average of the three measurements is also presented.

2.3 Dye concentration and COD analysis

The primary and residual color (after adsorption in different predefined conditions)

were measured using a spectrophotometer DR 5000 [16]. The maximum absorption of the dye AC 5R was at $\lambda_{max} = 574$ nm. Standard curve was plotted at this wavelength. Chemical oxygen demand (COD) was measured using the open reflux standard method 5220 B [17].

2.4 Response surface methodology

The initial dye concentration, pH and contact time parameters for maximum removal efficiency were optimized using central composite design (CCD) under response surface methodology (RSM). RSM was applied for the determination of simultaneous effects of pH (X1) initial AC 5R concentration (X2) and contact time (X3) on % COD removal (R1) and the AB113 remaining concentrations (R2).

The experimental variables and their ranges of variation are summarized in Table 1.

Table 1 Used independent variables and their ranges for experimental design

Variable	Unit	Range
Initial Dye Concentration	Mg l ⁻¹	5-50
pH	--	3-9
Time	Min	0-120

The total number of design points in the CCD was calculated by Eq. 2:

$$Eq. 2 \quad n = n_0 + 2k + 2^k$$

where n , k and n_0 are the number of required runs, number of factors and number of central points, respectively [18]. To determine the optimum values of the three selected factors, 20

$$Eq. 3 \quad R = b_0 + \sum_{i=1}^k b_i X_i + \sum_{i=1}^k b_{ii} X_i^2 + \sum_{i=1}^{k-1} \sum_{j=i+1}^k b_{ij} X_i X_j + \varepsilon$$

where R is the dependent variable, b_0 is constant value, b_i , b_{ii} and b_{ij} refer to the regression coefficient for linear, second order and interactive effects, respectively, X_i and X_j are the independent variables and ε is the error of

experiments were planned using a 23 full-factorial central composite design with 6 replicates at the central point.

A quadratic (second order) model as shown in Eq. 3 was used to estimate the interaction between dye removal and COD as responses (R) and three independent variables.

The CCD analysis and the associated statistical analysis were acquired using Design Expert 7.0.0 software. In Table 2, the actual and coded levels of the design are shown.

Table 2 Real and coded values of independent variables used for experimental design

Variables	Coded level				
	-alpha	-1	0	1	+alpha
	Real Values				
pH	3	4.216		7.784	9
Initial dye concentration	5	14.121		40.879	50
Time	0	24.324		95.676	120

MgO NPs were fixed on the glass using silicone adhesive. Ambient temperature were ranging from 18 to 25°C.

3. RESULTS

The design along with the removal efficiencies obtained is provided in Table 3. Accordingly,

COD removal efficiencies were between 0 and 99.35%, which was related to the run numbers 3 and 4, respectively. The findings of the study were in good agreement with those of Meriç et al. [19].

Table 3 central composite design and experimental results.

Run	Factor 1 A:pH	Factor 2 B: dye in	Factor 3 C:Time	Response 1 COD %Removal	Response 2 Remaining Dye, mg l ⁻¹
1	6	50	60	55.6453	22.65
2	6	28	60	39.1068	16.23
3	6	28	0	0	28.00
4	7.78	40	95.68	99.35	1.23
5	4.22	14	95.68	40.564	7.26
6	6	28	60	39.279	17.32
7	4.22	40	24.32	11.043	35.00
8	6	28	120	90.97	1.98
9	4.22	40	95.68	71.693	12.26
10	3	28	60	26.58	20.14
11	6	28	60	38.150	17.25
12	4.22	14	24.32	8.4107	12.84
13	7.78	40	24.32	20.63	31.75
14	6	5	60	15.156	4.65
15	9	28	60	51.39	13.98
16	6	28	60	40.696	16.45
17	7.78	14	24.32	12.664	12.30
18	6	28	60	40.3371	16.35
19	6	28	60	40.3422	16.85
20	7.78	14	95.68	51.4707	6.56

Neamtu et al. [20] reported 10 min as the optimum reaction time for the photo-Fenton process to the removal of 85% color and more than 90% COD removal. The comparison of the above-mentioned results with the current study showed similar findings at different contact times of dye and COD removal.

Analysis of variance (ANOVA) of quadratic model of COD removal efficiency and the remaining dye are presented in Tables 4 and 5, respectively. Based on the ANOVA results (Table 4 and Table 5), the effect of contact time was found to be the highest among the studied variables on COD and dye removal. In Table 4,

the model F-value of 705.12 indicated the model was significant. There was only 0.01% chance that the "model F-value" with this large size could occur due to noise. Also in Table 5, the model F-value of 518.65 implied the model was significant. There is only 0.01% chance that the "model F-value" with this large size could occur due to noise. The COD removal efficiency and remaining dye were close-fitting well to the quadratic model in the experimentations range of variables. A stepwise model reduction was done for COD removal and remaining dye concentrations models to omit the non-significant model terms and the

reduced model is shown in Eqs. 4 and 5, respectively. The graphical representation provides a method to visualize the relation between the response and experimental levels of each variable, and the type of interactions between the test variables.

The optimum value of each variable was located based on the hump in the three-dimensional plot or from the central point of the corresponding contour plot.

Response surface plot for the combined effect of pH and initial dye concentration on COD removal is demonstrated in Figure 2. As can be seen in this figure, the percent of dye removal was increased with the increase of the pH and initial dye dosage. COD removal was raised with the increase of pH and initial dye

concentration. According to Moussavi and Mahmoudi [12], MgO was effective for decolorization and COD removal.

It seems that the high dye and COD removal in the alkaline pH region was related to the high adsorption efficiency of azo dye with MgO nanoparticles at more basic pH [21] and near the point of zero charge pH (pH_{pzc}). The pH, at which the net surface charge is zero, is called the point of zero charge [22]. The MgO pH_{pzc} is about 12.4 [23], which indicates the adsorption ability of the surface. This means that the surface was not saturated by dye adsorption at the alkaline pH and stayed available for more dye fragments [24].

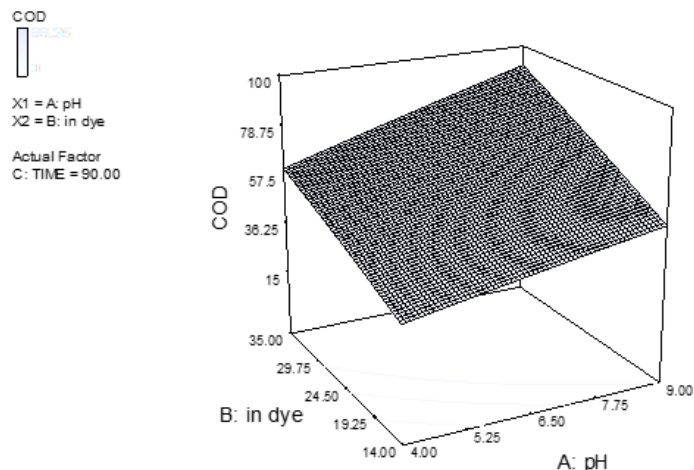


Figure 2 Response surface plot for combined effect of pH and initial dye concentration on COD removal efficiency.

Table 4 Analysis of variance (ANOVA) for Response Surface Reduced Quadratic Model of COD removal efficiency **

Source	Sum of Squares	df	Mean Square	F Value	p-value Prob > F	
Model	13047.31	8	1630.91	705.12	< 0.0001	significant
A-pH	661.78	1	661.78	286.12	< 0.0001	
B-initial dye	1816.23	1	1816.23	785.24	< 0.0001	
C-TIME	9743.17	1	9743.17	4212.40	< 0.0001	
AB	65.70	1	65.70	28.40	0.0002	
AC	80.63	1	80.63	34.86	0.0001	
BC	598.09	1	598.09	258.58	< 0.0001	
B ²	23.03	1	23.03	9.96	0.0092	
C ²	66.05	1	66.05	28.56	0.0002	
Residual	25.44	11	2.31			
Lack of Fit	20.72	6	3.45	3.65	0.0883	not significant

Pure Error 4.73 5 0.95

** Std. Dev.: 1.53, R-Squared: 0.9981, Adj R-Squared: 0.9966, Pred R-Squared 0.9866

Rotte et al. [21] showed that Safranin O dye adsorption on MgO decorated multi-layered graphene was increased by the pH increasing. They concluded with pH increase, $[H^+]$ plausibly decreased and resulted in less protonation of Safranin O dye, which in turn increased the adsorption of Safranin O onto the adsorbent.

Optimization and validation

To obtain the optimum condition through the model equation predicted by RSM, DesignExpert 7.0.0 software was applied using practical criteria. The criteria were maximum COD removal, minimum remaining dye dosage in the studied range (5–50 mg l⁻¹) and initial pH in the studied range (3–9). In the optimum conditions, all the factors concurrently met the predicted desirable criteria. Based on the assumptions noted, the predicted optimal conditions were initial dye of about 40 mg l⁻¹, pH of 8.9 and contact time of 90 min (COD removal efficiency 99.58%). To check the validity of the results expected by the model, additional laboratory experiments were conducted in 3 repetitions. Experimental data were in good consistency with those predicted through the regression model (97.56% vs. %99.58). According to the results, both predicted and experimental data were in close agreement and the most interesting finding was there was no significant difference between the results obtained experimentally. Rezaii Mofrad et al. [25] reported that optimum conditions of methyloange adsorption by MgO nanoparticles were 300 mg l⁻¹ initial dye concentration, 1.5 g l⁻¹ MgO and 10 min contact time. Although the optimum contact time obtained in the current study (90 min) was much more than the optimum contact time of the foresaid research (10 min), not using the high concentration of absorbent, no need for separating the nanoparticles and good performance at low dye concentrations were the advantages of this work.

4. CONCLUSION

The experimental study showed that fixed MgO on the glass was effective in AC 5R adsorption. Also, the results for COD removal were promising and more than 99% removal was achieved (Table 3). Therefore, another set of experimentations was planned with only effective factors, i.e. pH, initial dye and time, on the dye and COD. The experimental values obtained for the AC 5R removal efficiency were found to agree satisfactorily with the values predicted by the proposed model with a high coefficient of determination ($R^2 = 0.998$). The optimal operating point (initial dye: about 40 mg l⁻¹, pH: 8.9 and contact time: 90 min) giving maximum dye and COD removal was found using DesignExpert 7.0.0 software. The present results showed immobilized nanoMgO can be competitive with other processes such as photo Fentonin dye adsorption, but at higher contact time.

5. ACKNOWLEDGEMENT

The authors wish to thank Safety Promotion and Injury Prevention Research Center of Shahid Beheshti University of Medical Sciences for supporting this work under Research Fund grant. The work was carried out in the laboratories of the department of Environmental Health Engineering, school of Health, Shahid Beheshti University of Medical Sciences.

6. REFERENCES

1. Allen, S.J., McKay G., and Porter J.F., [2004]. Adsorption isotherm models for basic dye adsorption by peat in single and binary component systems. *Journal of Colloid and Interface Science*. 280(2): p. 322-333.
2. Dos Santos, A.B., Cervantes F.J., and van Lier J.B., [2007]. Review paper on current technologies for decolourisation of textile wastewaters: Perspectives for anaerobic biotechnology. *Bioresource Technology*. 98(12): p. 2369-2385.

3. Chowdhury, S., Mishra R., Saha P., and Kushwaha P., [2011]. Adsorption thermodynamics, kinetics and isosteric heat of adsorption of malachite green onto chemically modified rice husk. *Desalination*. 265(1–3): p. 159-168.
4. Verma, A.K., Dash R.R., and Bhunia P., [2012]. A review on chemical coagulation/flocculation technologies for removal of colour from textile wastewaters. *Journal of Environmental Management*. 93(1): p. 154-168.
5. Habiba, U., Islam M.S., Siddique T.A., Afifi A.M., and Ang B.C., [2016]. Adsorption and photocatalytic degradation of anionic dyes on Chitosan/PVA/Na–Titanate/TiO₂ composites synthesized by solution casting method. *Carbohydrate Polymers*. 149: p. 317-331.
6. Yagub, M.T., Sen T.K., Afroze S., and Ang H.M., [2014]. Dye and its removal from aqueous solution by adsorption: A review. *Advances in Colloid and Interface Science*. 209: p. 172-184.
7. Gupta, S.K., Singh J., Anbalagan K., Kothari P., Bhatia R.R., Mishra P.K., Manjuladevi V., Gupta R.K., and Akhtar J., [2013]. Synthesis, phase to phase deposition and characterization of rutile nanocrystalline titanium dioxide (TiO₂) thin films. *Applied Surface Science*. 264: p. 737-742.
8. Ghannadi, S., Abdizadeh H., and Golobostanfard M.R., [2014]. Modeling the current density in sol–gel electrophoretic deposition of titania thin film. *Ceramics International*. 40(1, Part B): p. 2121-2126.
9. Karaman, M., Saripek F., Köysüren Ö., and Yıldız H.B., [2013]. Template assisted synthesis of photocatalytic titanium dioxide nanotubes by hot filament chemical vapor deposition method. *Applied Surface Science*. 283: p. 993-998.
10. Guo, J., [2016]. Adsorption characteristics and mechanisms of high-levels of ammonium from swine wastewater using natural and MgO modified zeolites. *Desalination and Water Treatment*. 57(12): p. 5452-5463.
11. Mahmoud, H.R., Ibrahim S.M., and El-Molla S.A., [2016]. Textile dye removal from aqueous solutions using cheap MgO nanomaterials: Adsorption kinetics, isotherm studies and thermodynamics. *Advanced Powder Technology*. 27(1): p. 223-231.
12. Moussavi, G. and Mahmoudi M., [2009]. Removal of azo and anthraquinone reactive dyes from industrial wastewaters using MgO nanoparticles. *Journal of Hazardous Materials*. 168(2–3): p. 806-812.
13. Camtakan, Z., Erenturk S.A., and Yusan S.D., [2012]. Magnesium oxide nanoparticles: Preparation, characterization, and uranium sorption properties. *Environmental Progress & Sustainable Energy*. 31(4): p. 536-543.
14. Hu, J., Song Z., Chen L., Yang H., Li J., and Richards R., [2010]. Adsorption Properties of MgO(111) Nanoplates for the Dye Pollutants from Wastewater. *Journal of Chemical & Engineering Data*. 55(9): p. 3742-3748.
15. Balapure, K., Bhatt N., and Madamwar D., [2015]. Mineralization of reactive azo dyes present in simulated textile waste water using down flow microaerophilic fixed film bioreactor. *Bioresource Technology*. 175: p. 1-7.
16. Mahdavi, Y., Ghorzin F., and Sadeghi S., [2015]. Biosorption of acid blue 113 dyes using dried Lemna minor biomass. *Scientific Journal of Environmental Sciences*. 4(7): p. 152-158.
17. Federation, W.E. and Association A.P.H., [2005]. Standard methods for the examination of water and wastewater. American Public Health Association (APHA): Washington, DC, USA.
18. Khuri, A.I. and Mukhopadhyay S., [2010]. Response surface methodology. *Wiley Interdisciplinary Reviews: Computational Statistics*. 2(2): p. 128-149.
19. Meriç, S., Kaptan D., and Ölmez T., [2004]. Color and COD removal from

- wastewater containing Reactive Black 5 using Fenton's oxidation process. *Chemosphere*. 54(3): p. 435-441.
20. Neamtu, M., Yediler A., Siminiceanu I., Macoveanu M., and Kettrup A., [2004]. Decolorization of disperse red 354 azo dye in water by several oxidation processes—a comparative study. *Dyes and Pigments*. 60(1): p. 61-68.
 21. Rotte, N.K., Yerramala S., Boniface J., and Srikanth V.V.S.S., [2014]. Equilibrium and kinetics of Safranin O dye adsorption on MgO decorated multi-layered graphene. *Chemical Engineering Journal*. 258: p. 412-419.
 22. Boehm, H.P., [2002]. Surface oxides on carbon and their analysis: a critical assessment. *Carbon*. 40(2): p. 145-149.
 23. McCafferty, E., [1999]. A Surface Charge Model of Corrosion Pit Initiation and of Protection by Surface Alloying. *Journal of The Electrochemical Society*. 146 (8): p. 2863-2869.
 24. Talebian, N. and Nilforoushan M.R., [2010]. Comparative study of the structural, optical and photocatalytic properties of semiconductor metal oxides toward degradation of methylene blue. *Thin Solid Films*. 518(8): p. 2210-2215.
 25. Rezaii-Mofrad, M., Mostafaii G., Nemati R., Akbari H., and Hakimi N., [2016]. Removal of methyl orange from synthetic wastewater using nano-MgO and nano-MgO/UV combination. *Desalination and Water Treatment*. 57(18): p. 8330–8335.